Implications of the Born approximation for WEMVA - a systematic approach

Wiktor Weibull, and Børge Arntsen, Norwegian University of Science and Technology*

SUMMARY

Wave equation migration velocity analysis is an automatic iterative method for estimating seismic velocities from migrated images. The problem of obtaining velocity updates from images is currently solved by first expressing the object function perturbation as a linear function of the the model perturbations. And then solving the linear system using adjoint methods. Here we carefully analyse the errors associated with the linearization in the velocity analysis framework. The goal is to be able to quatify approximately what are the necessary conditions for a sucessful velocity inversion.

INTRODUCTION

The problem of estimating wave velocities for depth migration has traditionally been solved by seismic tomography using ray approximations. However, ray approximations have several shortcomings and often fail to be adequatelly accurate in areas with large and sharp velocity contrasts. To overcome this problem the velocity analysis method must include the whole wavefield. One such method is the wave equation migration velocity analysis (WEMVA). In recent years we have seen many successsful applications of WEMVA for imaging in areas of complex geological settings, such as subsalt (Sava and Biondi, 2004b) and through gas chimneys (Shen and Symes, 2008). In these applications WEMVA has shown to be superior when compared to ray tomographic methods.

Practical implementation of WEMVA is currently based on the Born approximation (Sava and Biondi, 2004a; Gao and Symes, 2009). Which means that successful implementation of the method must cope with the limitations imposed by this linearization. Despite this being a well known problem, it has not been systematicaly analysed in the framework of WEMVA. Here we present a quantitative analysis of the error associated with the Born approximation with respect to all parameters involved. This allows us to pinpoint what are the minimum necessary conditions for the velocity analysis to converge. We illustrate the implications of the non-compliance with these conditions with simple examples.

THEORY

First we develop the theory to the linearization of the objective function with respect to the model perturbations. Next we determine the error associated with the linearizations. We do this in the simple case of a constant background velocity medium, where the wave equation can be solved exactly. For notational purposes, the theory is developed for 2 dimensions (x_m, z), but it can easily be extended to 3D.

WEMVA is in essence an optimization procedure where the misfit to be minimized is a function of the migrated image. Minimization is sought through penalizing certain qualities of the image that are indicators of incorrect velocity, such as smearing of common image point gathers (Shen and Symes, 2008) or dip in angle domain common image point gathers (Sava and Biondi, 2004a). The following objective function illustrates how this can be defined:

$$M(s) = \frac{1}{2} \sum_z \sum_x \sum_h ||PR(x_m, h, z)||^2 \qquad (1)$$

Where $R(x_m, h, z)$ is the image volume, x_m are the subsurface midpoint coordinates, h can be either the subsurface offset or angle, and P is an operator which can be either a scaling by offset (h) or a derivation across angles ($\frac{\partial}{\partial \theta}$).

The slowness can be written as $\mathbf{s} = \mathbf{s}_0 + \Delta\mathbf{s}$, where $\mathbf{s}_0$ is the background slowness and $\Delta\mathbf{s}$ is an unknown slowness perturbation to be estimated. Equation 1 can be minimized through an iterative method, such as the Newton Rapson (Nocedal and Wright, 2000):

$$\Delta\mathbf{s}_{k+1} = [J^T J]^{-1} \nabla_s M(\mathbf{s}_{0_k}) \approx \alpha \nabla_s M(\mathbf{s}_{0_k}) \qquad (2)$$

Where k is the iteration index, alpha is the step size (diagonal approximation to the Hessian matrix), $\nabla_s M(\mathbf{s}) = J^T PR$, and $J = \frac{\partial}{\partial \mathbf{s}}(PR)$ is the Jacobian matrix.

We now analyse the error associated with the linear relation in equation 2 (Born approximation) by direct comparison with the exact solution to the wave equation in a constant background medium. The solution to the one way wave equation in a constant medium is given by Ursin (1984):

$$U(k_x, \omega, z) = \exp[-ik_z(z - z_0)] U(k_x, \omega, z_0) \qquad (3)$$

Where

$$k_z(k_x, \omega, s) = \sqrt{(\omega s)^2 - k_x^2} \qquad (4)$$

The variable k_x stand for the horizontal wavenumber in x_m direction. While ω is the angular frequency and s is the phase slowness $(1/v)$. For simplicity, from now on we omit dependence on k_x and ω.

Using equation 3 we can extrapolate a wavefield over a depth interval (Δz) using two slownesses (s_0 and $s_0 + \Delta s$). If we then subtract the resultant wavefields from one another, we end up with a wavefield perturbation due to a velocity perturbation (Δs) over a depth interval (Δz). In mathematical terms this is given by:

$$\begin{aligned} \Delta U_{z+\Delta z}(\Delta s) &= U_{z+\Delta z}(s_0 + \Delta s) - U_{z+\Delta z}(s_0) = \\ &= \left(e^{-ik_z \Delta z} - e^{-ik_{z_0} \Delta z}\right) U(z) \end{aligned} \qquad (5)$$

Where k_{z_0} and k_z are the vertical wavenumbers computed with s_0 and $s_0 + \Delta s$, respectively.

The linear relation between wavefield perturbation and slowness perturbation under the born approximation reads (Sava and Biondi, 2004a):

$$\begin{aligned}\Delta U_{z+\Delta z}(\Delta s) &\approx -i\Delta z \left.\frac{dk_z}{ds}\right|_{s_0} U(z)\Delta s \\ &\approx -i\Delta z \frac{\omega^2 s_0}{k_{z_0}} e^{-ik_{z_0}\Delta z} U(z)\Delta s \end{aligned} \quad (6)$$

The linearization space

Equation 6 is only valid for certain values of the variables k_x, ω, Δz and Δs, which makes it justifiable to truncate the Taylor series to the first order. In this section we are going to access under which circumstances can we use (6) to obtain a slowness perturbation given a wavefield perturbation.

We can compute the difference between the exact wavefield perturbation (5) and the linearized wavefield perturbation (6):

$$E = \left| 1 - e^{-i(k_{z_0}-k_z)\Delta z} + i\Delta z \Delta s \frac{\omega^2 s_0}{k_{z_0}} e^{i(k_{z_0}-k_z)\Delta z} \right| \quad (7)$$

We can call this the linearization error. This error is varying with the background velocity and velocity perturbation, but also with the frequency and wavenumber parameters. The error is divided by $U(z)$, to make it independent of the wavefield. The error is also normalized by $e^{-ik_z\Delta z}$, resuling in a relative error.

A better parametrization can be achieved if we use $\beta = \omega s_0 \Delta z$, $\rho = \frac{\Delta s}{s_0}$ and the planewave takeoff angle in the background medium (θ_0), where $\theta_0 = \arcsin\left|\frac{k_x}{\omega s_0}\right|$:

$$\begin{aligned} E(\beta,\rho,\theta_0) = \Big| 1 - e^{-i\beta(\cos\theta_0 - \sqrt{(1+\rho)^2 - \sin^2\theta_0}} \\ + i\frac{\beta\rho}{\cos\theta_0} e^{-i\beta(\cos\theta_0 - \sqrt{(1+\rho)^2-\sin^2\theta_0}} \Big| \end{aligned} \quad (8)$$

In this equation we take the slowness perturbation to be the absolute value of the perturbation, since a slowness perturbation can be either positive or negative.

Contour plots of the error in equation (8) for some values of parameters β, ρ and θ are shown in figure 1. From this figure, we can see that the error related to the linearization increases with increasing ρ, β and θ. For a fixed background slowness, this means that the error increases with the magnitude of the slowness perturbation, with the frequency and with the planewave takeoff angle. The error increase with these parameters occurs at an increasing rate until it finds inflection points. These inflection points indicate that the exact wavefield perturbation and the linearized wavefield perturbation are moving out of phase (cycle skipping).

Note that WEMVA is an iterative procedure, therefore large errors can be expected in the first iterations, which does not mean that the method will fail to converge. However cycle skipping represents a likelly failure of the inversion as it may cause the gradient of the objective function with respect to the slowness to point in the oposite direction of the minimum.

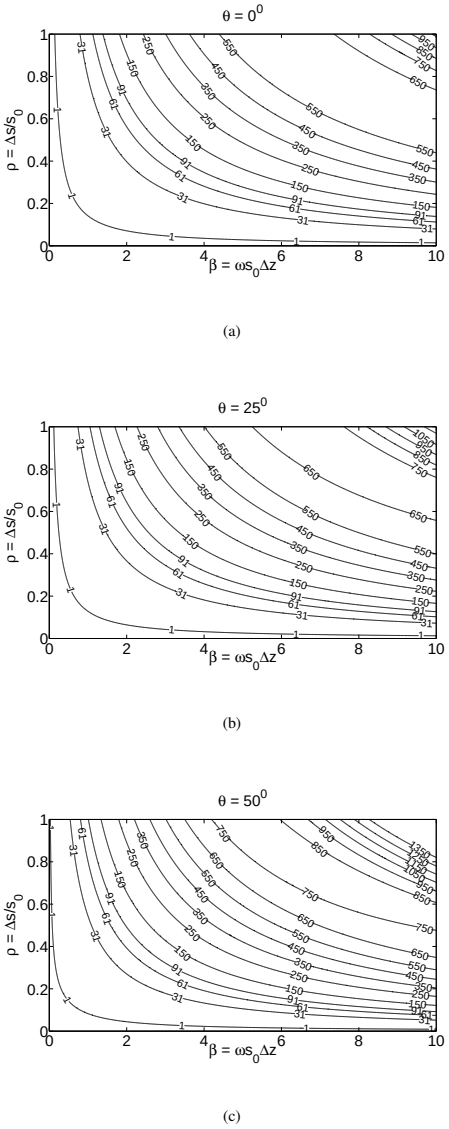

Figure 1: Contour plot of the linearization error (8) as a function of parametes ρ, β and θ.

Examples

To illustrate how this error analysis can be linked to the behaviour of WEMVA, we first show some simple examples in the framework of zero offset wave equation migration (Ursin, 1984). Next we show how error can affect convergence of WEMVA in a more practical example, where we are trying to minimize an objective function based on Differential Semblance Optimization (Symes and Carazzone, 1991; Shen and Symes, 2008).

In the first example we migrate a zero offset section represented by a broadband flat reflection at 1.6s. The migration is carried out with split-step fourier migration (Stoffa et al., 1990) under two different velocities, the correct velocity and a perturbed velocity. The two images are subtracted to obtain an image perturbation. We then use the adjoint state method (Plessix, 2006; Shen and Symes, 2008; Virieux and Operto, 2009) to produce a gradient of the image perturbation with respect to the slowness. In this process the adjoint of equation 6 is used. The maximum frequency content of the seismic data is 120 Hz, the background velocity is 1000 m/s, which corresponds to 500 m/s under the exploding reflector model (Ursin, 1984). The vertical extent is 5 m and the velocity perturbation is 450 m/s. This corresponds to values of β and ρ of 3.7 and 0.8, repectivelly. This values translate to an error of 360 % at $\theta = 0$, and as expected the gradient is completely wrong (fig. 2b-d). By comparison we show the result of a gradient computation with a maximum frequency of 30 Hz (fig. 2e-g). This gives a β value of .9 and albeit an error of 30 % at $\theta = 0$, the gradient is well behaved.

In the second example we migrate 200 synthetic common shot gathers taken over a model with flat reflectors and constant background velocity of 2000 m/s. Migration is again carried out with split-step fourier migration, using two slowness perturbations of different magnitudes, but located as in figure 3a. One perturbation has a magnitude of 80 m/s giving a β value of 19.6 and a ρ value of 0.04, which translates to a linearization error of 32 %. The other perturbation has magnitude of 420 m/s ($\rho = 0.26$) which gives an error of more than 600 %. For each case, we apply the offset imaging condition of Rickett and Sava (2002) to obtain an image volume ($R(x_m, h, z)$). And we compute the gradient of objective function (1) using the adjoint state method, as defined in Shen and Symes (2008). The result is shown in figure 3c-d. If the slowness perturbations were both compliant with the Born approximation, then both gradients would show similar behaviour. That is not the case, since we can clearly see that the gradient computed with the larger perturbation (fig. 3d) has oposite sign to the one computed with the smaller perturbation. This occurs despite the fact that the largest perturbation lies within the convex part of the objective function which contains the global minimum (fig. 3b).

DISCUSSION AND CONCLUSION

Equation 6, on which our error analysis is based, is valid for a constant background medium with lateraly homogeneous velocity perturbations. Several generalizations of this equation for laterally heterogeneous background medium and slowness perturbations exist. However all of these generalizations are based on approximations to the vertical wavenumber (k_z) and therefore we can expect that through averaging the background velocities and slowness perturbations our error analysis can be approximatelly applied also for heterogeneous mediums.

For examples 1 and 2 we used split-step fourier migration to be able to migrate data using velocity models with lateral slowness variations. Although this clearly breaks with the assumptions in our error analysis (slowness perturbations without lateral variations), it can be accomodated by using a mixed domain approach, as explained in Sava and Biondi (2004a). The experimental results show that the error analysis holds under these conditions. Note that background slowness is kept constant in all examples.

Our error analysis shows that success of WEMVA depends largelly on frequency content of the seismic signal, since the background slowness, slowness perturbations magnitude and extent are not known in beforehand. Another possibility to control the convergence of WEMVA would be to break down the model in depths steps and run WEMVA stepping down from top to bottom (shallow to deep areas). This way we can control the maximum extent of the perturbations, and avoid large errors in the deeper parts of the model.

ACKNOWLEDGMENTS

The authors acknowledge the financial support of Statoil and the sponsors of the ROSE consortium.

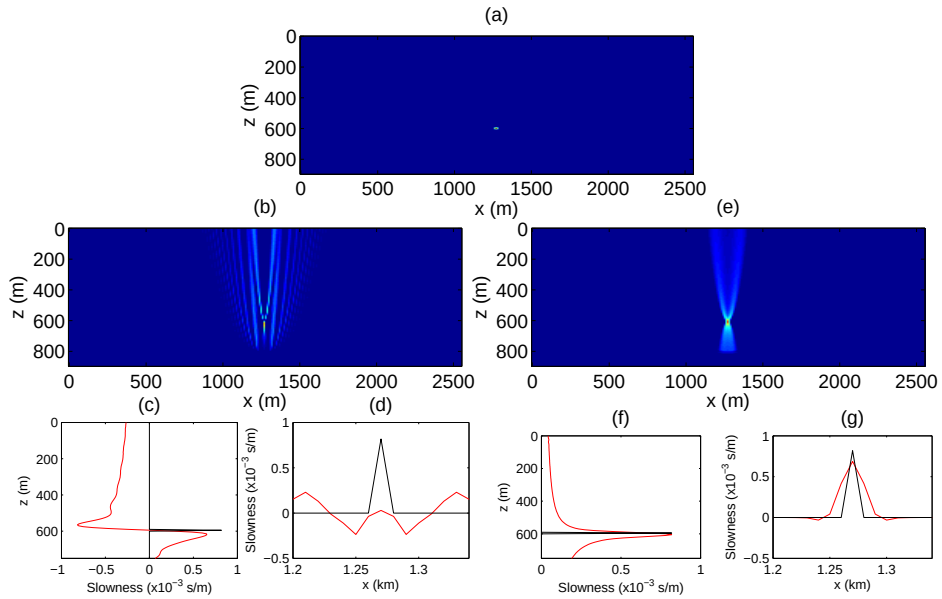

Figure 2: This figure shows a very simple example of the application of the linearization error to anticipate the behaviour of the first iteration of the WEMVA. a) Original slowness perturbation; b) Gradient with respect to the slowness of the image perturbation using 120 Hz maximum frequency; c) Vertical profile; d) longitudinal profile; e) Same as b) but now using a 30 Hz wavelet; f) vertical profile; g) longitudinal profile; Profiles are crossing the punctual slowness perturbation.

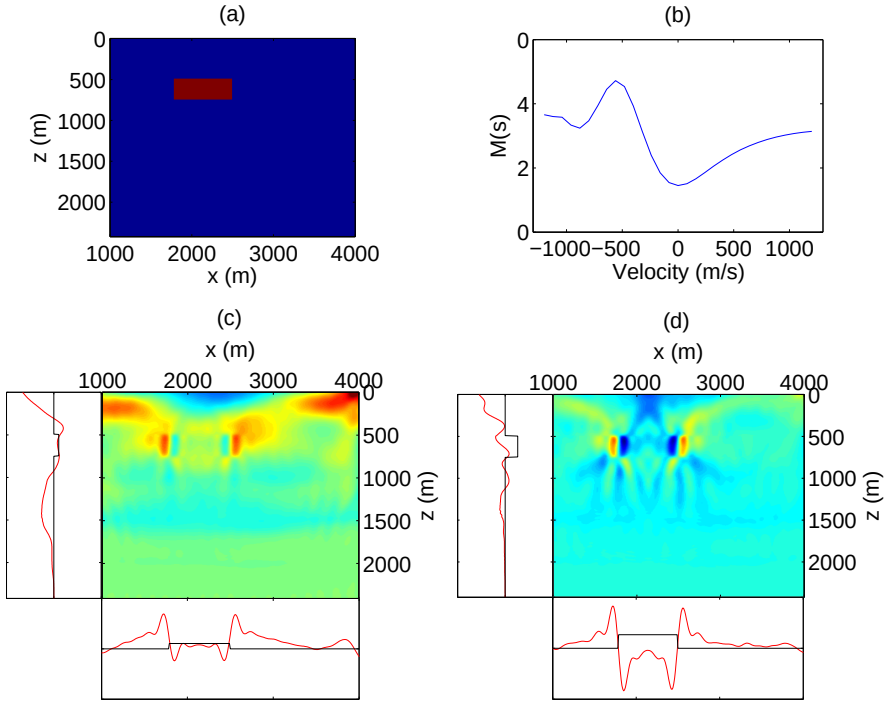

Figure 3: This figure shows a more practical example of the application of the linearization error to anticipate the behaviour of the first iteration of the WEMVA. a) Original slowness perturbation; b) Objective function (1) computed for various values of the slowness perturbation in a). c) Gradient computed with -80 m/s velocity pertubation; d) Gradient computed with -420 m/s velocity pertubation; Profiles accompanying the gradients are crossing in the middle of the slowness perturbation x= 2140 m and z= 620 m.

EDITED REFERENCES

Note: This reference list is a copy-edited version of the reference list submitted by the author. Reference lists for the 2010 SEG Technical Program Expanded Abstracts have been copy edited so that references provided with the online metadata for each paper will achieve a high degree of linking to cited sources that appear on the Web.

REFERENCES

Gao, F., and W. Symes, 2009, Differential semblance velocity analysis by reverse time migration: Image gathers and theory: SEG Technical Program Expanded Abstracts, **28**, 2317–2321.

Nocedal, J., and S. J. Wright, 2000, Numerical optimization: Springer.

Plessix, R. E., 2006, A review of the adjoint-state method for computing the gradient of a functional with geophysical applications: Geophysical Journal International, **167**, no. 2, 495–503, doi:10.1111/j.1365-246X.2006.02978.x.

Rickett, J. E., and P. C. Sava, 2002, Offset and angle-domain common image-point gathers for shot-profile migration: Geophysics, **67**, 883–889, doi:10.1190/1.1484531.

Sava, P., and B. Biondi, 2004a, Wave-equation migration velocity analysis, I. Theory: Geophysical Prospecting, **52**, no. 6, 593–606, doi:10.1111/j.1365-2478.2004.00447.x.

———, 2004b, Wave-equation migration velocity analysis, II: Subsalt imaging examples: Geophysical Prospecting, **52**, 231.

Shen, P., and W. W. Symes, 2008, Automatic velocity analysis via shot profile migration: Geophysics, **73**, no. 5, VE49–VE59, doi:10.1190/1.2972021.

Stoffa, P. L., J. T. Fokkema, R. M. de Luna Freire, and W. P. Kessinger, 1990, Split-step fourier migration: Geophysics, **55**, 410–421, doi:10.1190/1.1442850.

Symes, W. W., and J. J. Carazzone, 1991, Velocity inversion by differential semblance optimization: Geophysics, **56**, 654–663, doi:10.1190/1.1443082.

Ursin, B., 1984, Seismic migration using the WKB approximation: Geophysical Journal of the Royal Astronomical Society, **79**, 339–352.

Virieux, J., and S. Operto, 2009, An overview of full-waveform inversion in exploration geophysics: Geophysics, **74**, no. 6, WCC1–WCC26, doi:10.1190/1.3238367.